The significance of doping in enhancing polypyrrol nanofiber storage ability as a supercapacitor

H. O. A. Kareem[a,*], I. M. Ibrahim[b,*], S. J. Mohameed[c,*], F. J. Hameed[d,*]
[a]*Department of physics, College of education for pure Sciences, University of Tikrit, Tikrit, Iraq*
[b]*Department of physics, College of Science, University of Baghdad, Baghdad, Iraq*
[c]*Department of physics, College of education for pure Sciences, University of Tikrit, Tikrit, Iraq*
[d]*Department of physics, College of Science, University of Baghdad, Baghdad, Iraq*

Polypyrrol was prepared by electrochemical polymerization. Polypyrrol morphology has been investigated by FE-SEM and it shows a polypyrrol nanofibre network. By doping PPy nanofibers with different MW-CNT proportions (10%, 20%, 30%, 40% vol.ratio), nanocomposites were obtained. When adding MW-CNT with PPy, the nanotubes particles on the nanofibre network gradually grew in proportion to added ratio, and hence a clear change in the nanocomposite structure was observed. The electrochemical measurements indicate that the nanocomposites demonstrate strongly pseudocapacitive activity. The capacitance of pure PPy was (19.23 Fg-1), while the maximum value of capacitance (153 Fg-1) was observed when 30% MW-CNT was doped with pure PPy.

(Received February 28, 2021; Accepted April 15, 2021)

Keywords: Polypyrrole, MW-CNT nanoparticles, Nanocomposites of PPy/MW-CNT, Morphology, Electrochemical measurements, Pseudocapacitor

1. Introduction

Polypyrrole (PPy) is a typical electrical conductive polymer from the unique material class which combines metal and semiconductor properties [1], [2]. Among the many conductive polymers (PPy) and their derivatives attracted a great deal of attention due to their high electrical conductivity, good environmental stability and easy synthesis and processing[3]–[5]. As in most organic molecules, when the monomer is oxidized, pyrrole polymerisation occurs, which forms a conjugated polymer chain with π-orbitals alternating and a positive charge around the polymer backbone. [6], [7]. Several experiments on polypyrrole have been carried out since its fibrous structure, which is a high-capacity electrical substance, has a wide surface area. In both water and air systems, ease of preparation, intrinsic electrical conductivity and high flexibility make PPy a promising material. [8]–[11].

The supercapacitors are a new energy storage technology, also called electrochemical capacitors or ultracapacitors. Supercapacitors not only have rapid storage capabilities, but also have efficiently delivered electric energy. Supercapacitors have many benefits relative to other batteries, such as high power capacity, long working life, and low maintenance costs. Electrochemical capacitor has been a common energy storage system in recent years, consisting of electrode materials such as carbon materials, transition metal oxide and polymer conducting–[12] [17]. Due to its specific characteristics, such as high conductivity, fast charge-discharge mechanism, good thermal stability, low cost and high energy density, Polypyrrole (PPy) is one of the most promising p-type CPs for the Faradaic pseudocapacitor application. [18]–[22]. The PPy-based electrode's electrochemical activity also depends on the methods of electrode preparation and the effective surface area of the active electrode. A single-charge and multiple charge anion is usually doped with PPy [23]. CPs-based research has focused extensively on PPy for the

---

[*] Corresponding authors: omar.k.alfahdawe@gmail.com

preparation of the pseudocapacitor electrode through chemical or electrochemical pathways in recent years. In the presence of excess surfactants, chemical oxidation-polymerization can synthesize a large variety of PPy nanostructure[24] .

In this research, the PPy/MW-CNT nanocomposites composite was synthesized for supercapacitor use by chemical oxidation polymerization.

2. Experimental work

2.1. Materials used

($FeCl_3$) Iron(III) chloride (Thomas Baker. India), Methyl Orange (MO) (sigma chemical Co) and Multi Walled Carbon nano tubes (Sky Spring Nanomaterials, Inc. USA) (Pyrole monomer (Sigma Aldrich. China).

2.2. Synthesis of ppy nanofiber

During the procedure, 0.0818 g (2.5 mmol) of methyl orange (MO) was dissolved in (288 ml) cooled distilled water (5 °C) and combined with (1 ml, 14 mmol) pyrrole monomer, and the mixer was stirred (5min) until the mixture was fully melted and turned to red, at this point, the mixing phase is halted. In (33 ml) distilled water, (3.88 g) ($FeCl_3$) is dissolved and added drop by drop for two hours in a (MO-Pyrrole) cold solution. The reaction solution is placed in an ice bath and set on a stirrer and mixed for (24 hours). The precipitated PPy is then isolated by filtration and rinsing (water, acetonic alcohol) 2 times each stage, and then dried in an oven at 80 °C for 12 hours.

2.3. Functionalize of CNT

MW-CNT powder (20 mg) was dissolved in (20 ml) Dimethylformamide (DMF) and stirred for six hours, after which the solution was ultrasonic treated for 8 hours to obtain a homogenous solution.

2.4. Preparation of PPy/CNT nanocomposite

0.02g of CNT was dissolved in 20 ml (DMF), 0.04g of PPy was dispersed in 40 ml of distilled water, then different volume ratio of carbon nano tube where mixed with PPy (PPy/CNT, 9:1, 8:2, 7:3 and 6:4) ml. The resulting solution was sonicated for two hours in order to get a homogeneous dispersion ready for use.

2.5. Preparation of capacitor device

For this reason, (1×1) cm^2 nickel foam substance has been used. PPy and PPy/MW-CNT nanocomposite were deposited on it by drop casting technique to be ready for supercapacitor analysis, and put in 1 ml of (H_2SO_4) as well as to test the cyclic voltammetry (CV) curves, galvanostatic charge-discharge (GCD) measurements and electrochemical impedance spectroscopy (EIS) to determine its capacity.

3. Results and discussion

FE-SEM studied the morphological properties of composites. The FE-SEM images demonstrate the nanostructures of prepared materials. When the substance has been prepared using the process of chemical oxidation. The pure PPy layer structure was shown in (Fig. 1-a), where it clearly observe that the PPy layer is in the form of nanofibers structure, and the size of network fibers of PPy was less than 100 nm as can be seen in (Fig. 1-b). MW-CNT was tube-like in morphology and was also given in Fig (2-a, 2-b) (Dopant material). Less than 22 nm was the scale of the dopant materials. When we prepare the nanocomposites of PPy and MW-CNT nanoparticles at different rate of MW-CNT(10% , 20% , 30% , 40%), were seen that MW-CNT successfully grew on the surface of the PPy layer.

The PPy/MW-CNT morphology of composites is seen in Fig (3). From the FE-SEM images, it is clear that tube-shaped particles are evenly distributed on the surface of the polymer, due to of the MW-CNT were added, therefore Fig. 3a-d reveals a gradual rise in MW-CNT within polymer chains. It's obvious that MW-CNT on the conducting polymer matrix are uniformly distributed. This showed that the nanocomposites were effectively mixed and homogeneously combined, which would increase the surface area and produce superior capacitance.

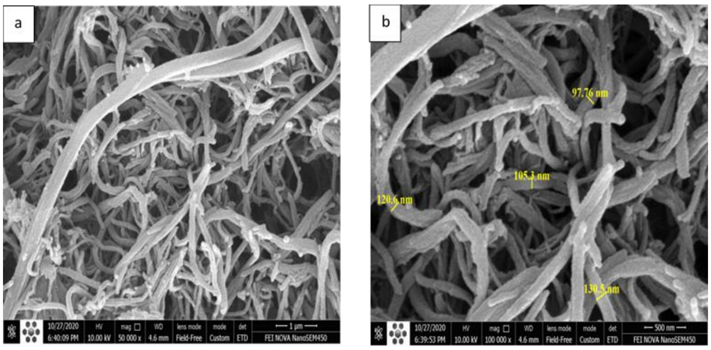

Fig. 1. (a , b) FE-SEM images of pure PPy nanofiberes at different magnification.

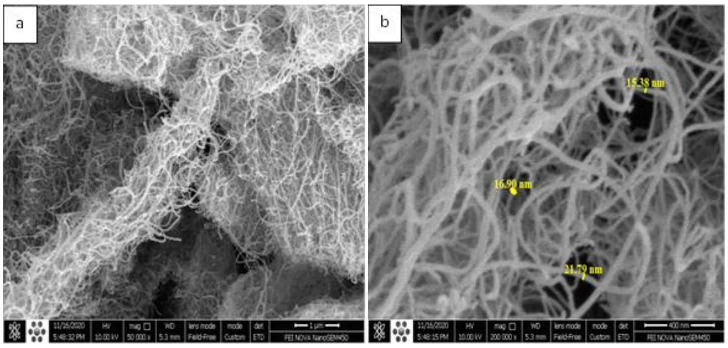

Fig. 2. (a, b) FE-SEM images of MW-CNT at different magnification.

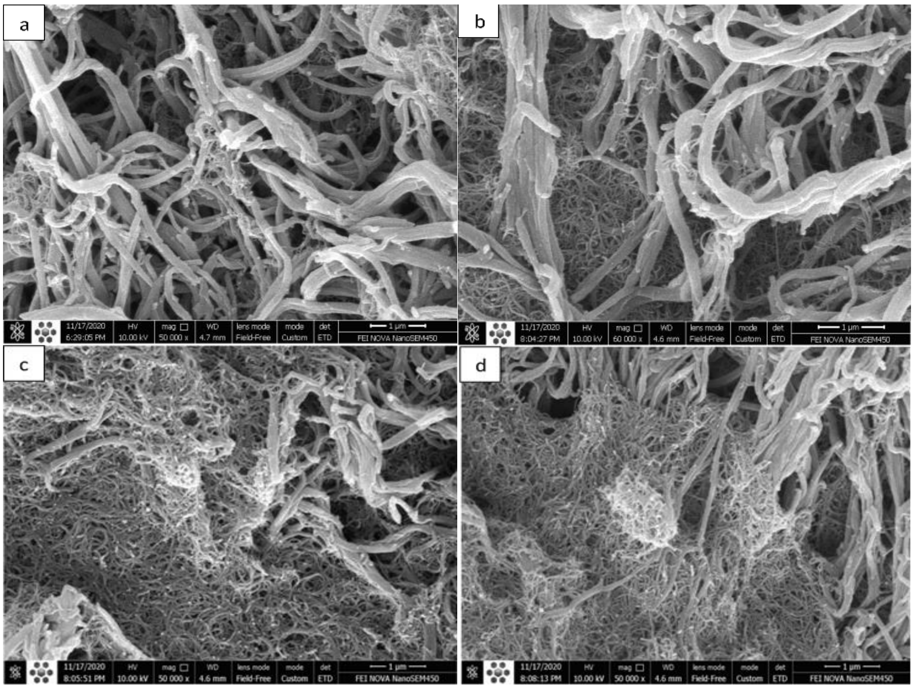

Fig. 3. (a , b, c, d) FE-SEM images of PPy / MW-CNT nanocomposites at different doping rates of CNT (a- 10% , b-20% , c-30% , d-40%).

The electrochemical properties of the PPy and PPy nanocomposites were characterized in the H_2SO_4 electrolyte. Electrochemical performance of PPy nanocomposite was examined by cyclic voltammetry (CV), galvanostatic charge/discharge (GCD), and electrochemical impedance spectroscopy (EIS) measurements. Where, the effect of doping PPy with different proportions of MW-CNT on the cyclic voltammetry (CV) and galvanic charge / discharge (GCD) curves and electrochemical impedance spectroscopy (EIS) results were studied in order to obtain the optimum electrochemical efficiency of PPy nanofibre electrode. Thus the PPy / MW-CNT composite film combines the benefits of carbon nanotubes and polypyrol. Electrochemical performance was firstly characterized using CV curves. Cyclic voltammetry (CV) curves of the fiber-shaped PPy/MW-CNT supercapacitor in 1.0 ml H_2SO_4 acid at 5 mV/s scan rates, as shown in (Fig. 4).

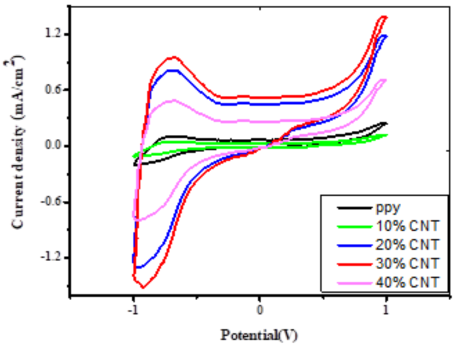

Fig. 4. CV curves of the PPy/MW-CNT composite film under different doping rate, at the scanning rate 5 mV s-1.

The PPy/MW-CNT CV curves revealed a pair of well-defined redox peaks at all doping levels due to the reversible faradic redox reaction. In the (CV) curves of the PPy/MW-CNT electrode, the pseudocapacitance activity was observed due to the influence of oxidation and reduction reactions. The anodic and cathodic peak potential changed in more positive and negative directions, respectively, with the increase in dopant rate, causing no noticeable change in the shape of the CV curves.

Scan rate and charge/discharge current are considered to be closely related to each other, i.e. higher scan rate produces higher current of charge/discharge. Redox reactions can also occur more thoroughly in PPy/MW-CNT supercapacitors at lower scan rates [25], [26].

This result shows the good rate capability of PPy /MW-CNT. The action of pseudocapacitance was also found in the GCD curves of PPy/CNT electrode within a potential window ranging from (0 – 0.4 V) at current of 2×10^{-3}, as shown in the (Figure: 6). Since carbon nanotubes are effective electron conductors, they can provide the electron transfer path of the composite and lead to rapid charge/discharge characteristics in the composite film. The average specific capacitance was determined according to equations (1) and (2) respectively from the CV curves and discharging curves.

$$\boldsymbol{C} = \frac{\int \boldsymbol{IdV}}{\boldsymbol{2m\Delta V\,v}} \tag{1}$$

$$\boldsymbol{C} = \frac{\boldsymbol{I\times\Delta t}}{\boldsymbol{m\times\Delta V}} \tag{2}$$

where: v is scan rate (mv/s), ΔV is voltage window , m is the mass of the electrode ≈ 0.5 mg/ cm^2, I is the applied current, Δt is the discharge current . In order to achieve the charge (Q), the capacitance was measured by integrating the area of the CV curve and then dividing the charge by the mass (m) of the electrode and the potential window 'V'. PPy/MW-CNT electrode outcomes have variable capacitances of 9.8 F g^{-1}, 129.6 F g^{-1}, 153 F g^{-1} and 78.2 F g^{-1} respectively at doping concentrations of (10 % , 20 %, 30 % and 40% MW-CNT).The basic capacitance of pristine PPy film, on the other hand, is only 19.5 F g^{-1} at 5 mV s^{-1}. This shows the capability of rapid charge/discharge and the composite film's good rate efficiency as a supercapacitor electrode. The electrochemical properties have been measured for different samples in order to determine the optimum preparation conditions and showed their unique capacitances at different doping levels (Fig. 5). The specific capacitance of the PPy/MW-CNT electrode showed an increase-and-decrease pattern with increasing carbon nano tube dopant, and we notice that when using dopant, the best preparation conditions are 30 percent MW-CNT.

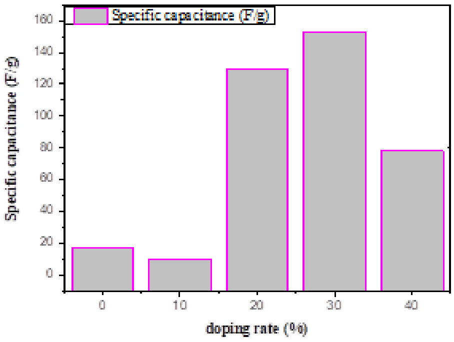

Fig. 5. Specific capacitance of the PPy/MW-CNT composite film at different doping rates.

In short, the mechanism of enhanced electrochemical efficiency of the composite film of PPy/MW-CNT is known to be the synergism between PPy and CNT [27]. Where carbon nanotubes include good conductivity, high specific surface area and good mechanical properties, PPy is high-capacity, low-cost and environmentally friendly. As a result, the composite film of the PPy/MW-CNTs shows good electrochemical efficiency, such as high capacity, quick charge/discharge ability, long cycling life, high energy and power density, so it is a suitable electrode material for high efficiency of supercapacitors.

In addition, galvanostatic calculation of charge/discharge was carried out to test electrochemical efficiency as well. (Fig. 6) displays at applied current 2×10^{-3}A the charge/discharge curves of the composite electrodes. While equivalent charge/discharge times imply excellent electrochemical reversibility, the shape of GCD curves over lower current densities means greater faradic contribution (redox reactions) to the charge accumulation mechanism [26], [28]. Notably, PPy/MW-CNT composite electrode has a larger specific capacitance of 142 F g^{-1} for PPy / 30% MW-CNT, in contrast to 37.74 F $g^{-1}$for pure PPy, 44.57 F g^{-1} for PPy doping with 10% MW-CNT, 138.18 F g^{-1} for 20% MW-CNT and 116.36 F $g^{-1}$for PPy/40% MW-CNT .These values are compared to the findings of the CV. In addition, at applied current densities, the voltage drop is small, indicating a low internal resistance for the composite electrode PPy/MW-CNT. Such a small internal resistance is very desirable for the delivery of high power. The carbon nano tube increases the rate of electrochemical reactions in PPy/MW-CNT composites and decreases the resistance to charge transfer [29]. Pseudocapacitive charge storage in PPy is therefore increased, providing high specific capacitance (142 F g^{-1}) at a doping rate of 30 percent CNT.

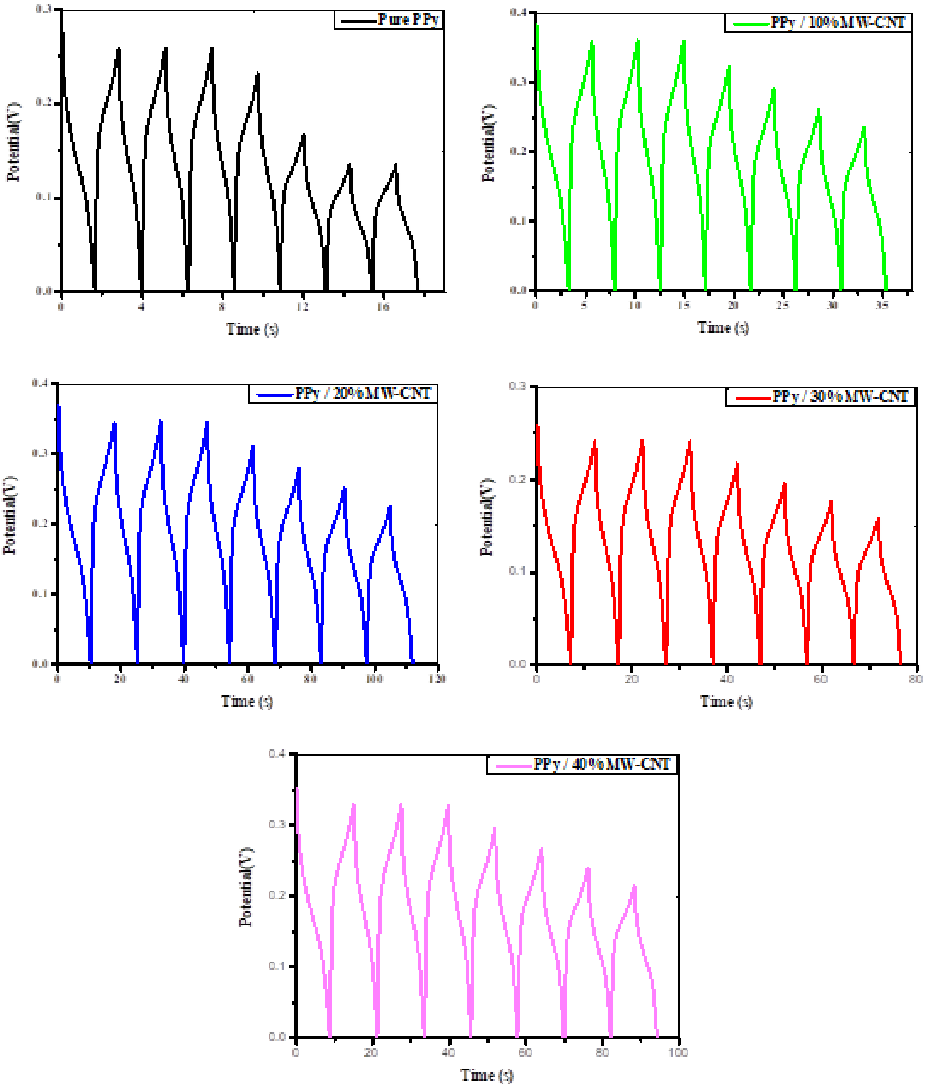

Fig. 6. Galvanostatic charge–discharge of PPy and PPy / MW-CNT electrode for supercapacitor.

The Nyquist plot was tested at the open circuit potential using a 5 mV amplitude AC voltage with a frequency range of 10 Hz to 200 kHz, (see Fig. 7). To understand the charge transfer of PPy / MW-CNT electrode material, the EIS plot was carried out on PPy samples and PPy / MW-CNT composites (Fig. 7). The ohmic resistance could be measured by actual part of impedance high frequency intercept of the semicircle. At higher frequencies, the small semi-circle shows a low transfer resistance of the charge with mild diffusion at lower frequencies. If the beeline displayed a slope of 45° at a low frequency region, the mechanism was driven by diffusion, it was strictly capacitive behavior if the slope was 90° in nature. The impedance map shows a semi-circular shape, indicating a very efficient transfer of charge. This finding further confirms the excellent stability of electrochemical cycling of PPy/MW-CNT nanocomposite, which has shown potential application as electrode material for electrochemical supercapacitors.

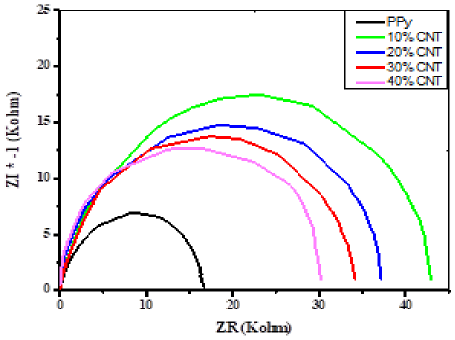

Fig. 8. Nyquist plots of the electrochemical impedance spectroscopy for the PPy, and PPy / MW-CNT.

4. Conclusions

In summary, PPy nanofiber and nanocomposite of PPy / MW-CNT have been prepared by simple method. The composite film of PPy and MW-CNT is a good electrode material for electrochemical supercapacitor. The maximum capacitance values (152 Fg^{-1}) that determined by CV curves were obtained from PPy nanofibers doped with 30% MW-CNT, but for pure PPy the capacitance is very small compared to PPy doping with MW-CNT. Therefore, doping plays a very important role in improving the capacitance of supercapacitor.

References

[1] M. Kolasińska, R. Krastev, P. Warszyński, Journal of colloid and interface science **305** (1), 46 (2007).

[2] N. S. Ilicheva, N. K. Kitaeva, V. R. Duflot, and V. I. Kabanova, ISRN Polymer Science **2012**, (2012).

[3] S. Sirivisoot, R. Pareta, T. J. Webster, Journal of Nanotechnology **22** (8), 85101 (2011).

[4] H. Yoon, Nanomaterials **3** (3), 524 (2013).

[5] J. Janata, M. Josowicz, Nature materials **2** (1) 19 (2003).

[6] A. Radi, S. Eissa, Electroanalysis **22** (24), 2991 (2010).

[7] S. A. Popli, U. D. Patel, Journal of Electrochemical Science and Engineering **5** (2), 45 (2015).

[8] S. Carquigny, O. Segut, B. Lakard, F. Lallemand, P. Fievet, Synthetic Metals **158** (11), 453 (2008).

[9] K. K. Kanazawa et al., Synthetic Metals **1** (3), 329 (1980).

[10] M. Nishizawa et al., Biomaterials **28** (8), 1480 (2007).

[11] A. Hamilton, The Formation and Characterisation of a Polypyrrole Based Sensor for the Detection of Urea, National University of Ireland Maynooth, 2012.

[12] L. Fan, L. Tang, H. Gong, Z. Yao, R. Guo, Journal of Materials Chemistry **22** (32), 16376 (2012).

[13] J. Tong et al., Journal of materials science **51** (4), 1966 (2016).

[14] H. Zhang, Y. Wang, C. Liu, H. Jiang, Journal of alloys and compounds **517**, 1 (2012).

[15] Q. Wu, M. Chen, K. Chen, S. Wang, C. Wang, and G. Diao, Journal of Materials Science **51**(3), 1572 (2016).

[16] Y. Yan, P. Gu, S. Zheng, M. Zheng, H. Pang, H. Xue, Journal of Materials Chemistry A **4**(48), 19078 (2016).

[17] J. Zhao et al., Progress in Natural Science: Materials International **26**(3), 237 (2016).

[18] L.-Z. Fan, J. Maier, Electrochemistry communications **8** (6), 937 (2006).

[19] H. An et al., Journal of Power Sources **195** (19), 6964 (2010).

[20] J. Wang, Y. Xu, J. Wang, X. Du, Synthetic Metals, **161**(11–12), 1141 (2011).

[21] L. Zhao, L. Zhao, Y. Xu, T. Qiu, L. Zhi, and G. Shi, Electrochimica Acta **55** (2), 491 (2009).

[22] K.-Y. Shen, C.-W. Hu, L.-C. Chang, K.-C. Ho, Solar energy materials and solar cells **98**, 294 (2012).

[23] S. Suematsu, Y. Oura, H. Tsujimoto, H. Kanno, K. Naoi, Electrochimica acta **45**(22–23), 3813 (2000).

[24] I. Shown, A. Ganguly, L. Chen, K. Chen, Energy Science & Engineering **3**(1), 2 (2015).

[25] Y. Chen, L. Du, P. Yang, P. Sun, X. Yu, W. Mai, Journal of Power Sources **287**, 68 (2015).

[26] R. Xu, F. Guo, X. Cui, L. Zhang, K. Wang, J. Wei, Journal of Materials Chemistry A **3**(44), 22353 (2015).

[27] X. Sun, Y. Xu, J. Wang, Journal of Solid State Electrochemistry **16**(5), 1781 (2012).

[28] S. Roldán, C. Blanco, M. Granda, R. Menéndez, R. Santamaría, Angewandte Chemie International Edition **50**(7), 1699 (2011).

[29] H. Fu, Z. Du, W. Zou, H. Li, C. Zhang, Journal of Materials Chemistry A **1**(47), 14943 (2013).